BRILL

IAWA Journal 42 (3), 2021: 279–298

iawa

Hydraulic function and conduit structure in the xylem of five oak species

Marta I. Percolla, **Jaycie C. Fickle**, **F. Daniela Rodríguez-Zaccaro**, **R. Brandon Pratt**, and **Anna L. Jacobsen***

Department of Biology, California State University, 9001 Stockdale Highway, Bakersfield, CA 93311, USA
*Corresponding author; email: ajacobsen@csub.edu

Accepted for publication: 19 March 2021

ABSTRACT

Many plant lineages, including oaks (*Quercus* spp.), have both vessels and tracheids as hydraulically conductive cells within their xylem. The structure of these co-occurring conduit types and their contribution to plant hydraulic function have been relatively little studied. We hypothesized that vasicentric tracheids contribute to hydraulic function under conditions of low water availability. We predicted that within a species, oaks growing at drier and warmer low elevation sites would have more tracheids and be more embolism resistant compared to those growing at moister and colder higher elevation sites. We also predicted that across species, lower elevation oaks would have increased tracheid abundance within their xylem. Five oak species differed in many xylem traits, including vessel diameter and length, tracheid size and abundance, embolism resistance, and hydraulic conductivity. Tracheids were most abundant in the xylem of the highest elevation species at sites that receive winter snow and freezing temperatures. Vessels were relatively vulnerable to embolism as confirmed with multiple methods, including centrifuge vulnerability curves, micro-CT scans of native stem samples, and single vessel air injection. Theoretical conductivity calculations indicated that tracheids account for 5.7–15.5% of conductivity in hydrated stems, with tracheids likely increasing in importance as large diameter vulnerable vessels embolize. The occurrence of both vessels and vasicentric tracheids in the xylem of oaks may enable them to function within highly seasonal climates. Tracheids, though often overlooked, may be particularly important in maintaining conductivity throughout much of the year when water potentials decline from seasonal maximums and following freeze-thaw events.

Keywords: Cavitation; embolism; HRCT; tracheid diameter; tracheid length; vessel diameter; vessel length; vulnerability to cavitation.

INTRODUCTION

Across the globe, reports of plant mortality and dieback due to water stress are abundant and have been linked to changing environments (Allen *et al.* 2010; Anderegg *et al.* 2016; Venturas *et al.* 2016). In the northern hemisphere, *Quercus* (oak) species found within many plant communities, represent important components of woody plant flora and are often dominant species within the communities in which they are found. In mediterranean-type climate regions, both shrub and tree oak species have experienced dieback and mortality with recent droughts (Paddock III *et al.* 2013; Brown *et al.* 2018; Jacobsen & Pratt 2018a; Batllori *et al.* 2020), with limited regeneration potential within stands for some of these species (Serra-Diaz *et al.* 2016). One predicted response to climate change in montane regions is that species will migrate upslope, tracking the conditions they are adapted to as lower elevations become warmer and drier. In this context, comparing species traits related to drought tolerance across elevation gradients is important for understanding how species might respond, including the potential for adaptation or acclimation.

Anatomically, axial hydraulic conductance within oak xylem occurs through vessel elements and vasicentric tracheids and may also include vascular tracheids. Vessel elements may be much wider in diameter than tracheids and vessel elements connect axially via simple perforation plates to form multi-celled vessels. Tracheids are generally narrower than vessels and lack perforations (e.g., they are 'imperforate'). Both vessels and tracheids contain lateral inter-conduit bordered pits with homogenous angiosperm-type pit membranes. Within vessel-bearing angiosperms, tracheids are often categorized according to their distribution within the xylem, with vascular tracheids occurring at the end of a growth ring in the latewood and

DOI 10.1163/22941932-bja10059

vasicentric tracheids occurring near and surrounding vessels and usually abundant within earlywood. Oaks frequently have both of these types of tracheids.

In the present study, we use the term tracheid to refer to the vasicentric and vascular tracheids within the xylem of our studied oak species. Tracheids were distinguished from libriform fibers within the xylem of our study species by the presence of relatively large and distinctly bordered pits. While these cell types were distinct and easily identified, the separation and associated terminology for differing types of imperforate tracheary elements is not uniform, types may intergrade, and some types may be difficult to distinguish within other taxa (Baas 1986; Carlquist 1986; Rosell *et al.* 2007). For simplicity, we generally use 'tracheid' throughout this text, and we refer specifically to vasicentric tracheids where appropriate. For other taxa, carefully distinguishing between tracheary element types is likely important in understanding how these cell types are functioning within the xylem (Olson *et al.* 2020).

Both vessels and tracheids may contribute to plant hydraulic function when they co-occur in the xylem. Vasicentric tracheids, as found in oaks, have been hypothesized to be particularly important for drought tolerance of arid and semi-arid adapted plants, because these tracheids could form a connected axial network among both each other and rare scattered functional vessels, thus maintaining a low level of hydraulic conductance during drought (Carlquist 1985; Carlquist & Hoekman 1985). This idea was also evaluated by Pratt *et al.* (2015) and species without tracheids were more vulnerable to drought-induced embolism compared to species with vasicentric tracheids, which had the most resistant xylem. Vasicentric tracheids may also contribute to hydraulic efficiency and the connectedness of the vascular network (Barotto *et al.* 2016).

The smaller diameter of tracheids relative to vessels is important in understanding how they contribute to hydraulic function. The direct relationship between the diameter of tracheary elements and hydraulic flow is mathematically explained by the Hagen-Poiseuille equation. This physical principle explains that the flow capacity of a conduit is directly related to its diameter raised to the fourth power (Tyree & Zimmermann 2002). Based on this principle, wider diameter vessels will account for a significantly larger proportion of hydraulic transport relative to narrow tracheids. Additionally, this difference may be compounded by the resistance to flow from the many pits that must be traversed between short imperforate tracheids as opposed to generally longer vessels. This additional resistance is not accounted for by the Hagen-Poiseuille equation (Sperry *et al.* 2005) nor are the other resistances encountered within the vessel network (Jacobsen & Pratt 2018b; Mrad *et al.* 2018).

During periods of water stress or following freeze-thaw stress, tracheids may be particularly important because their narrower diameter reduces their risk of hydraulic failure relative to co-occurring vessels. Many studies have found that risk of cavitation and embolism formation is linked to conduit diameter and this trend has been found in multiple species comparisons (Hargrave *et al.* 1994; Martinez-Vilalta *et al.* 2002; Jacobsen *et al.* 2016) and within species (Cai & Tyree 2010; Jacobsen *et al.* 2019). The risk of gas emboli formation with freeze-thaw cycles is directly linked to the diameter of the tracheary conduits within the xylem (Davis *et al.* 1999; Pittermann & Sperry 2003, 2006). Thus, narrow tracheids will be more likely to maintain water transport under both water stress and freeze-thaw conditions. Another possibility is that tracheids may not be particularly resistant to drought-induced embolism, but due to their abundant numbers, some of them may remain functional to keep axial hydraulic continuity to prevent vessels from becoming isolated (Jacobsen & Pratt 2018b).

In the present study, tracheid and vessel structure and hydraulic function were examined among and within five native oak species occurring along an elevation gradient in the southern Sierra Nevada Mountains of California, USA. The traits we focused on were chosen to yield insight into the drought tolerance of species across an environmental gradient. This is important because variation in drought tolerance traits may indicate that a species has the potential to adapt or acclimate to warming and drying climate conditions. We predicted that intra-specifically, oaks growing at drier and warmer low elevation sites would have more tracheids and be more embolism resistant compared to individuals of the same species found growing at higher elevation sites. We also predicted that among species, oaks that inhabit lower elevation habitats would have increased tracheid abundance within their xylem, with greater tracheid abundance favored because of their ability to tolerate the drier conditions. Several conduit structural and functional traits were examined in order to determine if these varied intra- and inter-specifically. Functional traits included measurements of vulnerability to embolism curves for all species at both their upper and lower distribution limits, as well as xylem-specific hydraulic conductivity. Structural traits included measurements of vessel and tracheid diameter and length, the abundance of vessel elements, tracheids, and fibers, and pit membrane area of inter-conduit bordered pits. Additionally, we used several different methods to evaluate hydraulic function measures and evaluate the potential functional roles of vessels and tracheids within oak xylem.

MATERIALS AND METHODS

Study sites and species

We examined five Californian native oak (*Quercus*) species of varying leaf habit, plant form, and distribution (Table 1). Five field sites were established within the Sequoia National Forest along a transect that spanned a large elevation gradient

Table 1.
California native oak (*Quercus*, Fagaceae) species included in the present study varied in leaf habit (evergreen, deciduous), growth ring porosity of mature xylem (ring or diffuse-porous), plant form (shrub, tree), elevation distribution (upper and lower distribution range) within California as reported by Baldwin *et al.* (2012), and vegetation community type in which they occurred (FW, foothill woodland; C, chaparral; MCF, mixed conifer forest) along a transect in the southern Sierra Nevada mountains of California, USA.

Species	Abbr.	Common name	Plant form	Leaf habit	Growth ring porosity	Community	Elevation range (m)
Q. chrysolepis Liebm.	Qc	Canyon live oak	Shrub to tree	Evergreen	Diffuse	C, MCF	30–2750
Q. douglasii Hook. & Arn.	Qd	Blue oak	Tree	Deciduous	Ring	FW, C	<1590
Q. garryana Hook.	Qg	Oregon oak	Shrub to tree	Deciduous	Ring	C, MCF	90–2140
Q. kelloggii Newb.	Qk	California black oak	Tree	Deciduous	Ring	MCF	30–2660
Q. wislizeni A. DC.	Qw	Interior live oak	Shrub	Evergreen	Diffuse	FW, C	<1600

Figure 1. Sites, where oaks were sampled, spanned a large elevation gradient in the southern Sierra Nevada mountains of California, USA, including low elevation foothill woodland (a), foothill woodland with mixed chaparral (b), low elevation chaparral (c), high elevation chaparral (d), and high elevation mixed conifer forests (e).

(823–1981 m) in the southern Sierra Nevada Mountains, California, USA (Fig. 1, Table 2). Sites were selected to include the lower (low site) and upper (high site) distribution of all oak species along this gradient. At each site, six individuals of each of

Table 2.
Study sites from which oak species were sampled in the present study, including the elevation of the site, the vegetation community type, and the common co-occurring woody species.

Site	Elevation (m)	Community type	*Quercus* spp.	Co-occurring species
1	823	Foothill woodland	*Q. douglasii* *Q. wislizeni*	*Ceanothus cuneatus* *Pinus sabiniana* *Rhamnus ilicifolia*
2	1304	Foothill woodland and mixed chaparral	*Q. douglasii* *Q. wislizeni*	*Ceanothus cuneatus* *Pinus sabiniana* *Rhamnus ilicifolia*
3	1356	Low elevation chaparral	*Q. chrysolepis* *Q. garryana*	*Arctostaphylos viscida* *Ceanothus cuneatus* *Cercocarpus betuloides* *Fremontodendron californica* *Garrya flavescens* *Rhamnus ilicifolia*
4	1707	High elevation chaparral	*Q. chrysolepis* *Q. garryana* *Q. kelloggii*	*Arctostaphylos viscida* *Cercocarpus betuloides* *Fremontodendron californica* *Garrya flavescens* *Rhamnus ilicifolia*
5	1981	Mixed conifer forest	*Q. kelloggii*	*Abies concolor* *Calocedrus decurrens* *Pinus ponderosa*

the oak species that occurred there were tagged so that they could be repeatedly sampled. At the lowest elevation sites, oaks formed the dominant woody components of the community, at mid-elevations they occurred as emergent elements within a shrub community, and at higher elevations, the oak species were co-dominant components within a mixed forest. The five species that were examined represent all of the locally occurring oak species.

Weather and soil data were examined from all sites. Long-term weather data were obtained from a local remote automated weather station (RAWS) at the low site and Parameter-elevation Regressions on Independent Slopes Model (PRISM) data for the upper sites. These data were supplemented by locally installed temperature and humidity dataloggers (Onset, HOBO MX2305, Onset Computer, Bourne, MA, USA) and manual rain gauges at all sites during the period of the study. In the time frame of the present study, weather data were examined from November 2017 to June 2018.

Soil samples were also collected to characterize each site. These samples were collected along with the organic matter atop the largely inorganic soil layer. Three soil samples were collected from each site near tagged plants and samples were collected from all 5 sites (i.e., 15 soil samples total). Samples were sent to USU Analytical Labs (Utah State University, Logan, UT, USA) for testing.

The water status of plants was also assessed seasonally (wet season, dry season). Water potential (Ψ_w) was measured on four small branchlets or leaves from six individuals of each species at both their upper and lower elevation distribution sites using a pressure chamber (Model 2000 Pressure Chamber Instrument, PMS Instruments, Corvallis, OR, USA). Sampling occurred in November 2017 (dry) and June 2018 (wet), and leaves were measured at both midday and predawn. Leaves were not bagged prior to their collection and these values thus represent the water potential of potentially transpiring leaves and not the water potential of the xylem (Pratt *et al.* 2020a).

Hydraulic conductivity and vulnerability to embolism

Vulnerability to water-stress-induced embolism was measured on the tagged individuals of each species (n = 6 per site per species) in June–July 2017 using a standard centrifuge method with hydration reservoirs (Tobin *et al.* 2013). For all plants, large branches ($\geqslant$1 m) were cut under water in the field. The cut ends of the harvested branches were kept under water, and branches were double bagged with large plastic bags before being transported to the laboratory at California State University, Bakersfield. Branches were refrigerated until they were processed for measurements within two days of harvesting. The large branches were cut underwater from both ends until a 14 cm long unbranched segment was obtained. We targeted stem

segments that were approximately 6 mm in diameter. Stem ends were shaved underwater, using a fresh razor blade, for each sample.

Conduit structure can vary with distance from stem apices (Olson & Rosell 2013; Olson *et al.* 2020). We did not specifically control for distance from stem tips, so there was some variability in sample distance from apices among our samples; however, sampling distance variation was relatively narrow, and our sampling protocol resulted in samples being collected from 20–50 cm from branch apices. Samples were collected from locations that met our target diameter while maximizing the distance of the selected sample from the basal end of our large, harvested branches. We did not notice obvious differences between species in stem taper or thickness. Cambial age may also impact xylem structure (Rodríguez-Zaccaro *et al.* 2019) and, following hydraulic measures, stem cross-sections were prepared and used to count the annual growth rings for each stem.

Stem segments were flushed with 20 mM degassed KCl solution at 100 kPa for 1 h to remove native emboli present within xylem vessels. Maximum hydraulic conductivity (K_{hmax}) was measured gravimetrically using a conductivity apparatus (Sperry *et al.* 1988). Maximum xylem-specific hydraulic conductivity (K_s) was calculated by dividing K_{hmax} by the xylem cross-sectional area of the distal end of the samples. Stem samples were spun in a centrifuge in a custom rotor with hydration reservoirs to induce water stress at successively more negative xylem pressure potentials, with hydraulic conductivity (K_h) measured between each spin (Alder *et al.* 1997; Tobin *et al.* 2013). Vulnerability to embolism curves for each sample were constructed by setting the K_{hmax} value for each sample at −0.5 MPa instead of 0 MPa to account for potential cavitation fatigue (Hacke *et al.* 2001). This step assumes that older and current year xylem that naturally embolized in the intact plant is damaged and that the spin at −0.5 MPa removes this population of non-functional xylem from the analysis. Xylem vulnerability to embolism was compared using the pressure at which 50% and 90% K_h had been lost (P_{50} and P_{90}, respectively). These parameters were calculated for each sample using a Weibull curve (Microsoft Excel 2010, Microsoft, Redmond, WA, USA).

Leaf-specific hydraulic conductivity (K_{leaf}) was calculated for each sample by measuring all of the leaf area distal to the stem segment measured for K_{hmax} (LI-3100 Area Meter, LI-COR, Lincoln, NE, USA). Leaf-specific conductivity was calculated as the K_{hmax} divided by the total distal leaf area. These leaves were then dried in an oven at 60°C for >2 days and their mass determined using an electronic balance. Specific leaf area (SLA) was calculated as the leaf area per dry leaf mass.

Evaluation of vessel vulnerability to embolism and hydraulic methods

To determine the validity of the centrifuge method used to generate vulnerability curves, we used different and independent methods on a subset of species. The first test involved using high-resolution computed tomography (micro-CT) scans of native stems from two species, *Q. garryana*, and *Q. kelloggii*, to generate single-point estimates that could be compared to vulnerability curve estimated values for the same pressures. For these samples, six large branches were collected from tagged plants in the field. The branches were >2 m long and were cut in air from the plant. These branches were then double bagged in large plastic bags and transported to a lab where they were left to equilibrate for >2 h. At least 4 small branchlets or leaves were harvested, and their water potential measured using a pressure chamber.

For five of these large branches, an intact branch apex approx. 50 cm in length was then carefully cut from the larger branch under water and was placed into the micro-CT scanner (Skyscan 2211, Bruker, Kontich, Belgium). During the scan, the cut end of the sample remained in water and the distal end remained intact and wrapped in plastic film to stabilize and prevent transpiration. From these scans, the proportion of vessels that were filled with gas and water were calculated and used to calculate the percentage of gas-filled conduits.

For the sixth large branch, and as an additional examination of conductivity patterns, we used a conductivity tracer to identify conductive conduits. The end of a large branch of *Q. kelloggii* was cut successively under water and then the end was placed into a container of an X-ray dense iodine solution following the methods of Pratt & Jacobsen (2018). This tracer has been shown to be an effective tracer of conductive xylem conduits. The branch was then allowed to transpire for 3 hrs before being bagged to equilibrate and then processed as described above.

As an additional test, we used single vessel air injection (SVAI) to measure the air-seeding pressure of current year vessels in *Q. douglasii* and compared this to a centrifuge-based hydraulic vulnerability curve measured on the current year xylem of paired samples collected at the same time from the same individuals. Stem segments used for this experiment were from different individuals than those used for the upper and lower site comparison and were collected specifically for this test (n = 5 individuals sampled). For SVAI, emboli were removed from samples by submerging them in 20 mM KCl and vacuum infiltrating (−91 kPa) them for 1 h. SVAI methods follow those described by Venturas *et al.* (2016) in which each xylem segment was secured vertically under a stereo microscope (Olympus, Tokyo, Japan) with the proximal end submerged in degassed 20 mM KCl solution. A glass capillary was inserted into a single vessel within the outer growth ring and the other end of the capillary was connected via tubing to a pressure chamber that was used to slowly increase the pressure within the vessel.

Open vessels, those with no terminal vessel elements in the sampled stem segment, had bubbles emerge at very low pressure (<0.05 MPa) and these were excluded from measures. From each individual tree, the SVAI of 20 vessels was measured from the current-year growth of several different xylem segments, for a total of 100 vessel measures. The proximal sample end was observed until a pressure was reached that resulted in bubbles emerging from a vessel or vessels. This indicated that gas had been seeded through a pit membrane of the injected vessel. Paired samples were measured using the centrifuge hydraulic methods described above, with a slight modification; the inner growth rings of these samples were sealed with cyanoacrylate resin so that only their outer growth ring was being measured (Rodríguez-Zaccaro *et al.* 2019).

Tracheid abundance and size

Vessel element and tracheid abundance were determined from samples of macerated xylem. A 1 cm section of stem was removed from the end of each of the samples that were used for the hydraulics measures. The bark and pith were removed and the remaining xylem pieces were placed in vials with 20 mL of Jefferey's solution (1:1 10% chromic acid and 10% nitric acid; Franklin 1945). Samples were left in vials at room temperature for 2–4 days. The maceration solution was carefully decanted, and the samples were washed several times with DI water. Samples were suspended in 5 mL DI water, stained with Safranin O, and dehydrated with 70% ethanol solution prior to being mounted onto slides for examination.

For each sample, slides were photographed at 50× magnification using a microscope attached to a digital camera (Axio Imager. D2, AxioCam MRc, and AxioVision AxioVs40, v. 4.8.2.0, Carl Zeiss MicroImaging, Göttingen, Germany). Cells with thick secondary cell walls were well preserved within the macerations and easily identified. For each sample, 8 random slide views were photographed and the libriform fibers, tracheids, and vessel elements within each view were counted. At least 100 and up to 662 cells were counted per sample, with an average of 372 cells per sample and over 16 700 cells counted across all samples. These counts were used to calculate the percentage of fibers, tracheids, and vessel elements. For some sample macerations, preparation resulted in cells becoming degraded and fragmented. These samples were discarded, resulting in a final sample size of between 4 and 6 samples per site and species.

Higher magnification images were taken for measures of tracheid dimensions using the same microscope. For each species at both their upper and lower distribution sites, between 19 and 41 (average of 31) tracheids were photographed at higher magnification and their length and diameter were measured. These values were pooled for a given species and site.

Vessel diameters, lengths, and pit characteristics

After measuring stem samples for xylem hydraulic function, stems were frozen until processed for additional xylem anatomical features. For vessel diameter measures, thin cross-sections were made using a sledge microtome (Model 860 Microtome, American Optical, Buffalo, NY, USA) and mounted on slides with glycerol. For each sample, several images were taken with a digital camera (AxioXam MRc, Carl Zeiss MicroImaging) mounted on a light microscope (Axio Imager. D2, Carl Zeiss MicroImaging GmbH, Gottingen, Germany). Vessel lumen areas for at least 100 vessels were measured using an image analysis program (AxioVision, Axio Vs40, v. 4.8.2.0, Carl Zeiss MicroImaging). Identification of vessels within cross-sections was informed by vessel features and distributions as obtained from macerations (see above) and silicone injection of vessels (see below). Vessel diameters were obtained from lumen areas by calculating an equivalent circular diameter.

Thin longitudinal sections were made by hand using Teflon-coated razor blades (GEM single-edge stainless-steel Teflon-coated blades, No. 71970 Electron Microscopy Sciences, Hatfield, PA, USA). Sections were mounted on slides with glycerol. Pit-field areas were identified within vessels and multiple pit fields were selected from different vessels within the section to analyze (Axio Imager. D2, AxioCam MRc, and AxioVision AxioVs40, v. 4.8.2.0, Carl Zeiss MicroImaging). At least 12 pits were measured within each pit-field area and at least 6 pit fields from different vessels were analyzed. These values were used to calculate the mean individual pit membrane area and the percentage of the pit-field wall area that was composed of pit membrane.

Branches from tagged individuals were collected for vessel length measurements in November-December 2017. Large branches (>2 m long) were collected from the field, double bagged, transported to CSUB, and refrigerated until processed within 3 days of collection. In the laboratory, 50 cm stem segments of similar diameter and sample location to those collected for hydraulics measures were excised underwater and flushed with degassed 20 mM KCl solution at 100 kPa for 1 h to fill embolized xylem vessels. Stem segments were injected with a two-part silicone mixture (RhodorsilRTV-141, Rhodia USA, Cranbury, NJ, USA) containing a UV dye (Uvitex OB, Ciba Specialty Chemicals, Basel, Switzerland) dissolved in chloroform (1% by weight) into the basal end at 50 kPa for 24 h. After silicone injection, stems were cured at room temperature for >72 h. To rehydrate stem tissue for sections, stems were submerged in water for at least one week. Thin cross-sections were made using a sledge microtome (Model 860 Sledge Microtome, American Optical) at 0, 0.7, 1.4, 2.9, 5.8, 11.8, 24, and 48 cm and analyzed as described in Jacobsen *et al.* (2019).

Analyses

Hydraulic traits between the upper and lower elevation of sites for each species were compared using a two-way ANOVA with species (*Q. douglasii*, *Q. wislizeni*, *Q. chrysolepis*, *Q. garryana*, *Q. kelloggii*) as a random factor and distribution along the elevation gradient (low, high) as a fixed factor. Tukey's post hoc analyses were used to compare species. Within a species, upper and lower elevation distributions were compared using contrasts of within-species variation of xylem anatomical and functional traits. When data did not meet the assumptions of statistical tests, they were transformed as needed. This included a log-transformation of the absolute values for P_{50} data. The proportion of theoretical conductivity contributed by vessels and tracheids was calculated for each sample using the Hagen-Poiseuille relationship in which conductivity through a conduit is proportional to the radius of the conduit to the fourth power, measured vessel and tracheid diameters, and the relative abundance of vessel elements and tracheids from macerations. Relationships between traits were evaluated using Pearson correlations of species mean values from each site. All statistical analyses were conducted using Minitab (v. 17.2.1, Minitab, State College, PA, USA).

RESULTS

Characteristics of sites along an elevation transect

Climate varied along the transect, with the lower elevation site experiencing hotter temperatures, lower relative humidity, and lower precipitation than the upper elevation site (Fig. S1 in the Supplementary Material at 10.6084/m9.figshare.14380733). Soil texture was generally similar along the transect, with most soils categorized as loam (Table S1 in the Supplementary Material at 10.6084/m9.figshare.14380733). Individuals occurring at the high and low sites of a species distribution also differed in their water status, particularly for predawn and midday water potentials during the dry season (Table 3). Species also differed in their minimum water potentials, with the lowest water potentials in one of the low elevation species and the highest water potentials in one of the high elevation species. However, this pattern was complex and species with similar distributions, such as *Q. douglasii* and *Q. wislizeni*, also differed in their water potentials (Table 3).

Species differed in hydraulic conductivity and vulnerability to embolism

Different species had similar vulnerability to embolism curve shapes and were all relatively vulnerable to embolism (Fig. 2). The samples had high initial K_s and exhibited steep losses in conductivity with declining water potential. Species differed significantly from one another in their hydraulic function, including differing in P_{50}, P_{90}, and K_s (Table 4). The species that was the most resistant to embolism was *Q. wislizeni*, while *Q. garryana* and *Q. kelloggii* were the most vulnerable species; *Q. garryana* displayed the highest K_s (Table 5). There were no changes in hydraulic function between low and high elevation sites within a species (Fig. 2, Table 5), except for *Q. douglasii*, which was more vulnerable to embolism at higher elevation. The age of stem segments that were sampled for hydraulic measures was 6.06 ± 0.43 years (mean ± 1 SE) with individual samples containing xylem ranging from 3–15 years in age; age variability among samples was due to differences in growth ring width since samples were selected in the field based on their stem diameter. Xylem diameter of sampled stems was 5.61 ± 0.10 mm

Table 3.
Mean (± 1 SE) for seasonal maximum (Max.) and minimum (Min.) predawn (Ψ_{pd}) and midday (Ψ_{md}) water potentials of five oak (*Quercus*) species from high and low elevation sites for each species along a transect in the southern Sierra Nevada Mountains of California, USA.

Species	Site	*n*	Max. Ψ_{pd} (MPa)	Dist.	Spp.	Max. Ψmd (MPa)	Dist.	Spp.	Min. Ψpd (MPa)	Dist.	Spp.	Min. Ψmd (MPa)	Dist.	Spp.
Q. chrysolepis	High	6	−0.950 ± 0.026	n.s.	A	−2.036 ± 0.116	n.s.	A	−2.206 ± 0.284	*	B	−3.010 ± 0.191	*	A
	Low	6	−0.927 ± 0.076			−2.097 ± 0.050			−1.117 ± 0.099			−2.375 ± 0.200		
Q. douglasii	High	6	−0.703 ± 0.361	n.s.	A	−2.261 ± 0.034	*	B	−2.072 ± 0.210	n.s.	BC	−3.736 ± 0.196	n.s.	C
	Low	6	−0.879 ± 0.037			−2.808 ± 0.093			−1.649 ± 0.158			−3.860 ± 0.167		
Q. garryana	High	6	−1.077 ± 0.145	*	A	−2.157 ± 0.066	n.s.	A	−2.785 ± 0.117	*	C	−3.367 ± 0.078	n.s.	B
	Low	6	−0.631 ± 0.030			−2.142 ± 0.044			−2.140 ± 0.227			−3.254 ± 0.056		
Q. kelloggii	High	4	−1.041 ± 0.033	n.s.	A	−1.603 ± 0.069	*	A	−1.662 ± 0.090	n.s.	B	−2.133 ± 0.133	*	A
	Low	6	−1.083 ± 0.061			−2.275 ± 0.044			−1.632 ± 0.165			−2.654 ± 0.058		
Q. wislizeni	High	6	−0.929 ± 0.096	n.s.	A	−2.238 ± 0.042	n.s.	A	−1.140 ± 0.182	n.s.	A	−2.749 ± 0.167	n.s.	A
	Low	6	−0.909 ± 0.034			−2.088 ± 0.153			−0.847 ± 0.162			−2.735 ± 0.152		

To the right of each column comparisons between high and low sites for a species are presented (Dist.), with n.s. indicating no difference and * indicating a difference ($P < 0.05$) between high and low sites. Results are also reported for a comparison of species values (Spp.) for each trait; different letters indicate significant differences among species.

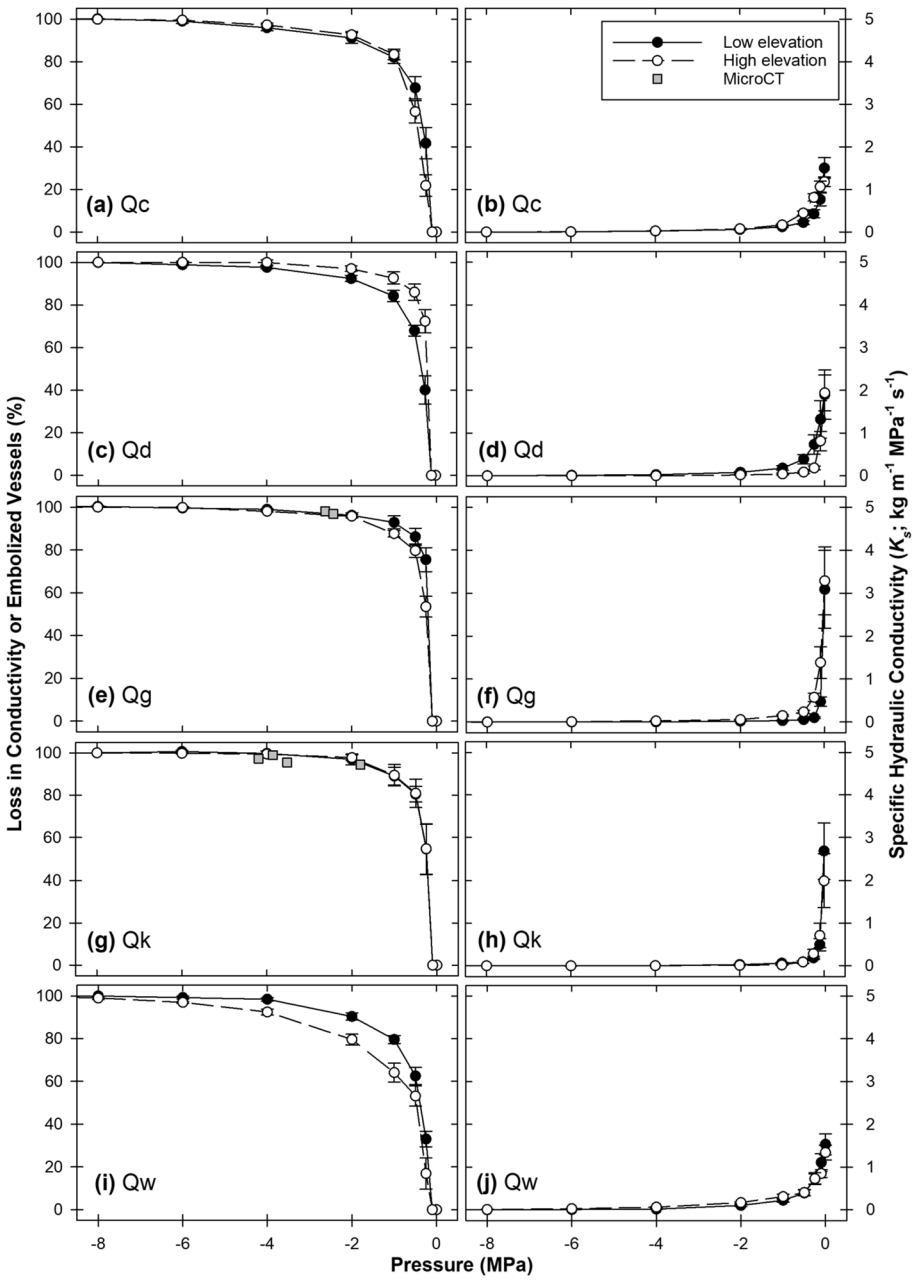

Figure 2. Vulnerability to embolism curves of stems from sites at the low and high elevation distribution for five oak species along a transect in the southern Sierra Nevada. Curves were generated using the standard centrifuge method and both the percentage loss in conductivity (a, c, e, g, i) and xylem specific hydraulic vulnerability (b, d, f, h, j) are shown. Percentage of embolized vessels as determined from micro-CT scans of large branches at native water potentials collected from trees along the transect and included for two species, *Q. garryana* (e) and *Q. kelloggii* (g).

(mean ± 1 SE). Species differed in their SLA (Table 5), but species did not differ in their overall leaf size except for *Q. kelloggii*, which had larger leaves than the other species (Table S2 in the Supplementary Material at 10.6084/m9.figshare.14380733). There were no differences among species in K_{leaf} (Table 5).

Comparison of hydraulic, micro-CT, and SVAI methods

Tests using independent methods were similar to hydraulic vulnerability curves, particularly in showing that vessels were highly vulnerable to embolism. Micro-CT scans of native branches showed the presence of numerous gas-filled (embolized) vessels, even at relatively high water potentials (Fig. 3). The percentage of embolized conduits of micro-CT samples was very similar to the PLC from vulnerability curves, with both indicating that samples were highly embolized with large losses in

Table 4.
Results from a mixed model analysis of variance (ANOVA) with species (*Q. chrysolepis*, *Q. douglassii*, *Q. garryana*, *Q. kelloggii*, *Q. wislizeni*), site along the elevation gradient (low or high elevation), and the interaction between the terms for several xylem structural and functional traits, including xylem vulnerability to cavitation (P_{50} and P_{90}), xylem-specific hydraulic conductivity (K_s), leaf-specific hydraulic conductivity (K_{leaf}), specific leaf area (SLA), and seasonal maximum (Max.) and minimum (Min.) predawn (Ψ_{pd}) and midday (Ψ_{md}) water potentials.

Trait category	Trait(s)	Species	Site	Interaction
Hydraulic function	P_{50}	$F_{4,59} = 13.48, P < 0.001$*	$F_{1,59} = 3.18, P = 0.080$	$F_{4,59} = 3.88, P = 0.008$*
	P_{90}	$F_{4,59} = 12.69, P < 0.001$*	$F_{1,59} = 1.23, P = 0.274$	$F_{4,59} = 3.43, P = 0.015$*
	K_s	$F_{4,59} = 3.86, P = 0.008$*	$F_{1,59} = 0.31, P = 0.578$	$F_{4,59} = 0.20, P = 0.938$
	K_{leaf}	$F_{4,59} = 2.03, P = 0.104$	$F_{1,59} = 1.28, P = 0.263$	$F_{4,59} = 1.23, P = 0.310$
Leaf structure	SLA	$F_{4,59} = 61.70, P < 0.001$*	$F_{1,59} = 0.21, P = 0.652$	$F_{4,59} = 1.27, P = 0.296$
Water status	Max. Ψ_{pd}	$F_{4,59} = 1.18, P = 0.333$	$F_{1,59} = 0.41, P = 0.523$	$F_{4,59} = 1.55, P = 0.201$
	Max. Ψ_{md}	$F_{4,59} = 15.49, P < 0.001$*	$F_{1,59} = 19.44, P < 0.001$*	$F_{4,59} = 10.35, P < 0.001$*
	Min. Ψ_{pd}	$F_{4,57} = 16.89, P < 0.001$*	$F_{1,57} = 17.86, P < 0.001$*	$F_{4,57} = 2.25, P = 0.077$
	Min. Ψ_{md}	$F_{4,57} = 26.69, P < 0.001$*	$F_{1,57} = 0.06, P = 0.811$	$F_{4,57} = 3.59, P = 0.012$*
Xylem structure	Vessel element (%)	$F_{4,41} = 1.90, P = 0.128$	$F_{1,41} = 0.07, P = 0.791$	$F_{4,41} = 1.35, P = 0.207$
	Tracheid (%)	$F_{4,41} = 4.70, P = 0.003$*	$F_{1,41} = 0.36, P = 0.550$	$F_{4,41} = 0.66, P = 0.624$
	Fiber (%)	$F_{4,41} = 4.83, P = 0.003$*	$F_{1,41} = 0.24, P = 0.628$	$F_{4,41} = 0.65, P = 0.629$
	Mean vessel lumen diameter	$F_{4,59} = 8.24, P < 0.001$*	$F_{1,59} = 0.34, P = 0.562$	$F_{4,59} = 0.34, P = 0.852$
	Maximum vessel lumen diameter	$F_{4,59} = 16.36, P < 0.001$*	$F_{1,59} = 0.01, P = 0.916$	$F_{4,59} = 0.46, P = 0.764$
	Mean vessel length	$F_{4,58} = 9.12, P < 0.001$*	$F_{1,58} = 1.39, P = 0.244$	$F_{4,58} = 1.64, P = 0.179$
	Pit membrane area	$F_{4,59} = 2.72, P = 0.040$*	$F_{1,59} = 0.01, P = 0.915$	$F_{1,59} = 1.28, P = 0.291$
	Tracheid diameter	$F_{4,299} = 9.72, P < 0.001$*	$F_{1,299} = 0.31, P = 0.5786$	$F_{4,299} = 2.77, P = 0.027$*
	Tracheid length	$F_{4,299} = 6.34, P < 0.001$*	$F_{1,299} = 3.22, P = 0.0739$	$F_{4,299} = 1.85, P = 0.119$

Values with an asterisk indicate those with a significant effect ($P < 0.05$).

conductivity (Fig. 2). A micro-CT scan of a stem that had been fed an iodine solution revealed that most vessels were non-conductive and were embolized, a few vessels were conductive, and large regions of the xylem contained tracheids that were conductive (Fig. 3b).

Older xylem may become more vulnerable over time in a process termed fatigue. Consequently, a separate test was conducted using SVAI and a centrifuge-based hydraulic vulnerability curve of only the current-year xylem. Both SVAI and this hydraulic vulnerability curve showed the same pattern as measures from multi-year samples, with conductivity declining rapidly with increasing pressure and current-year vessels that were highly susceptible to air-seeding (Fig. 4). The median vessel air-seeding pressure was 0.13 MPa with a lower and upper 95% confidence interval of 0.07 and 0.18 MPa, respectively. For samples from the same individuals measured at the same time, the hydraulic vulnerability curve of the current year xylem had a P_{50} of −0.44 MPa ± 0.14 (mean ± 1 SE).

Vessel and tracheid structure, abundance, and theoretical conductivity

All species contained vessels, tracheids, and libriform fibers within their xylem (Fig. 5). The structure of xylem conduits differed among the species in all measured structural traits, including vessel length and lumen diameter, tracheid length and diameter, and pit membrane area. Species did not differ in the proportion of vessel elements within their xylem but did vary in the abundance of tracheids and libriform fibers (Table 4). A general pattern that emerged from these differences was a separation of the two evergreen and diffuse-porous oaks, *Q. chrysolepis* and *Q. wislizeni*, from the other species (Tables 6 and 7). A second pattern among the deciduous species was for the species occurring at the lowest elevations, *Q. douglasii*, to differ from the species occurring at the highest elevation, *Q. kelloggii*, as was apparent in pit membrane area, the proportion of tracheids and fibers in the xylem, and also SLA. Vessel and tracheid structural traits and abundance did not generally differ within species between high and low sites (Tables 6 and 7). An exception to this was differences in tracheid diameter and length for *Q. chrysolepis* between the high and low sites. Representative micrographs of the different species from cross-sections and macerations are included in the Supplementary Material at 10.6084/m9.figshare.14380733 (Figures S2–S4). Vessels with relatively narrow diameters were often observed in samples. Narrow vessel elements could be recognized in macerations, where vessel elements were identifiable by their perforations. Narrow vessels were also apparent in silicone injections. Narrow diameter

Table 5.
Means (± 1 SE) of pressure at which 50% (P_{50}) and 90% (P_{90}) loss of conductivity occurred for stem segments, stem-specific hydraulic conductivity (K_s), leaf-specific hydraulic conductivity (K_{leaf}), and specific leaf area (SLA) of from sites at the high and low elevation distribution for each of five oak (*Quercus*) species.

Species	Dist.	*n*	Stem age (years)	P_{50} (MPa)	Dist.	Spp.	P_{90} (MPa)	Dist.	Spp.	K_s (kg s^{-1} m^{-1} MPa^{-1})	Dist.	Spp.	K_{leaf} (kg s^{-1} m^{-2} MPa^{-1})	Dist.	Spp.	SLA (mm^2 mg^{-1})	Dist.	Spp.
Q. chrysolepis	High	6	5.0 ± 0.5	−0.492 ± 0.047	n.s.	BC	−1.098 ± 0.160	n.s.	B	1.180 ± 0.112	n.s.	B	0.032 ± 0.005	n.s.	A	5.009 ± 0.225	n.s.	D
	Low	6	4.7 ± 0.7	−0.397 ± 0.050			−1.107 ± 0.286			1.503 ± 0.244			0.053 ± 0.012			4.702 ± 0.315		
Q. douglasii	High	6	7.2 ± 0.7	−0.243 ± 0.012	*	AB	−0.410 ± 0.106	*	AB	1.940 ± 0.421	n.s.	AB	0.121 ± 0.053	n.s.	A	7.910 ± 0.258	n.s.	C
	Low	6	6.8 ± 0.7	−0.378 ± 0.039			−0.963 ± 0.125			1.898 ± 0.577			0.436 ± 0.274			7.644 ± 0.224		
Q. garryana	High	6	5.2 ± 0.5	−0.288 ± 0.025	n.s.	A	−0.560 ± 0.113	n.s.	A	3.290 ± 0.793	n.s.	A	0.155 ± 0.045	n.s.	A	9.868 ± 0.277	n.s.	B
	Low	6	8.7 ± 1.3	−0.237 ± 0.013			−0.398 ± 0.092			3.091 ± 0.910			0.135 ± 0.030			8.741 ± 0.660		
Q. kelloggii	High	6	6.8 ± 1.7	−0.308 ± 0.043	n.s.	AB	−0.532 ± 0.153	n.s.	A	1.995 ± 0.626	n.s.	AB	0.088 ± 0.020	n.s.	A	10.506 ± 0.650	n.s.	A
	Low	6	6.5 ± 0.4	−0.283 ± 0.042			−0.388 ± 0.053			2.682 ± 0.655			0.055 ± 0.017			11.314 ± 0.893		
Q. wislizeni	High	6	4.5 ± 0.8	−0.670 ± 0.103	n.s.	C	−2.237 ± 0.499	n.s.	C	1.339 ± 0.174	n.s.	B	0.089 ± 0.018	n.s.	A	5.531 ± 0.113	n.s.	D
	Low	6	5.3 ± 0.6	−0.440 ± 0.031			−1.233 ± 0.151			1.532 ± 0.244			0.133 ± 0.037			5.775 ± 0.169		

The sample size (*n*) and mean (± 1 SE) age of sampled stems are also included. To the right of each column comparisons between high and low sites for a species are presented (Dist.), with n.s. indicating no difference and an asterisk (*) indicating a difference ($P < 0.05$) between high and low sites. Results are also reported for a comparison of species values (Spp.) for each trait; different letters indicate significant differences among species.

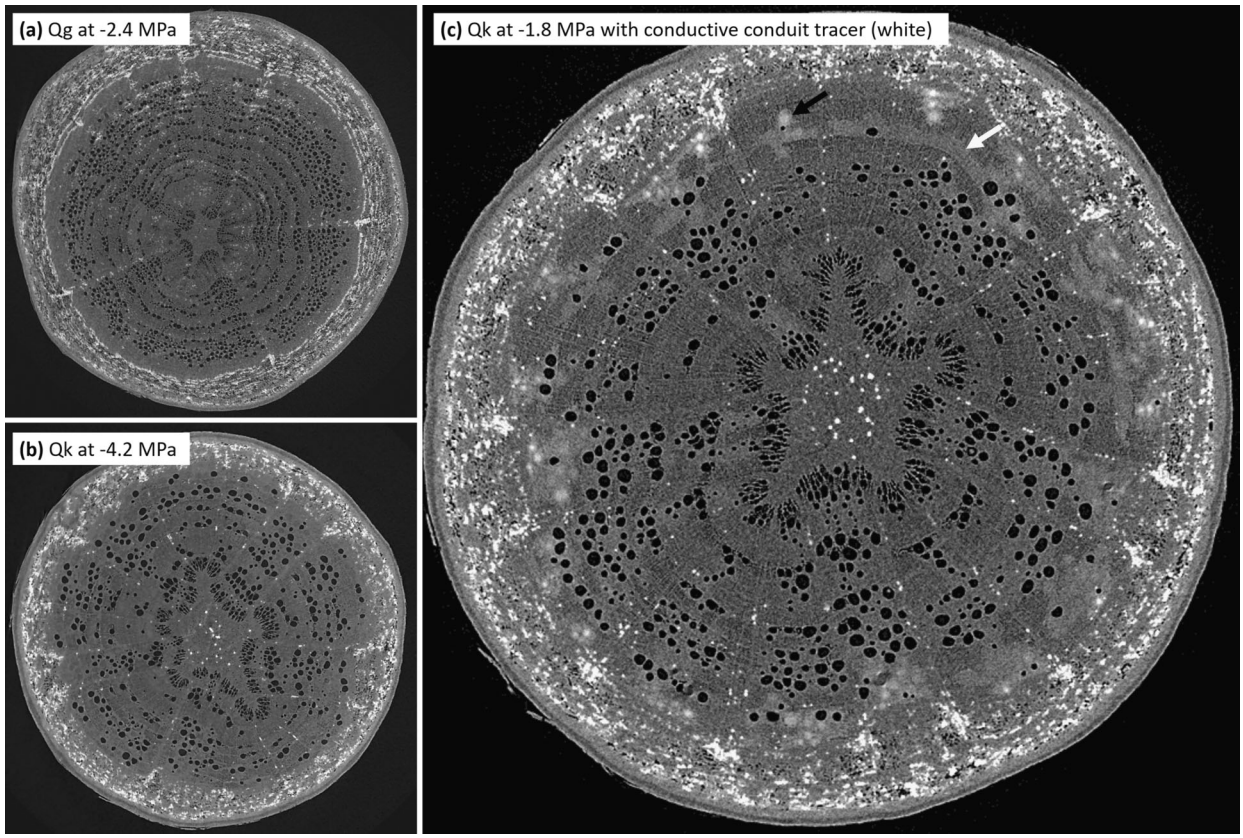

Figure 3. Representative micro-CT images of large branches collected during the summer dry season from the studied plants. Water-filled vessels are dark grey and embolized vessels that contain gas are black (a, b); stem xylem vessels were highly embolized. A native stem of *Q. kelloggii* was fed an x-ray dense solution into its cut end to mark the conduits and regions of the stem that were conductive following the protocol described in Jacobsen and Pratt (2018) (c). For this stem, conductive conduits are visible as lighter grey within the xylem. Nearly all vessels within the xylem are embolized (black); an example conductive vessel is indicated with a black arrow. Tracheids within the xylem were conductive as indicated by the light grey region early in the outer growth ring, with a representative region indicated with a white arrow. Some tracheid-based conductivity is also apparent within older growth rings. Bright white spots in the pith, xylem, and bark are naturally occurring crystals.

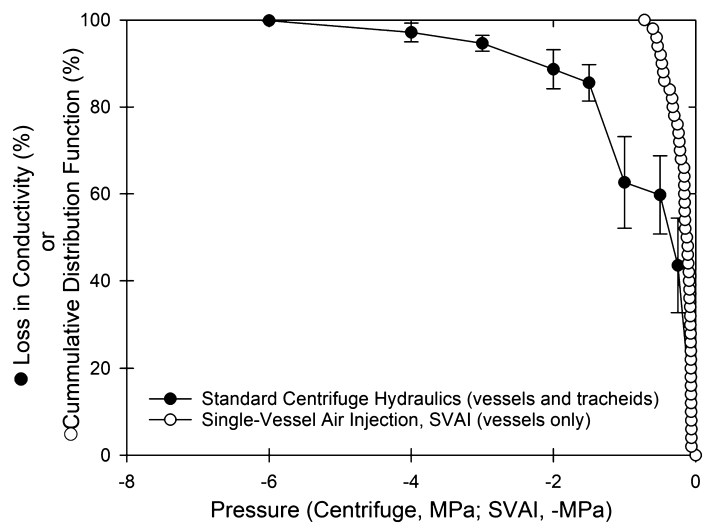

Figure 4. Vulnerability curves from standard centrifuge and single vessel air injection (SVAI) methods for samples of *Quercus douglasii*.

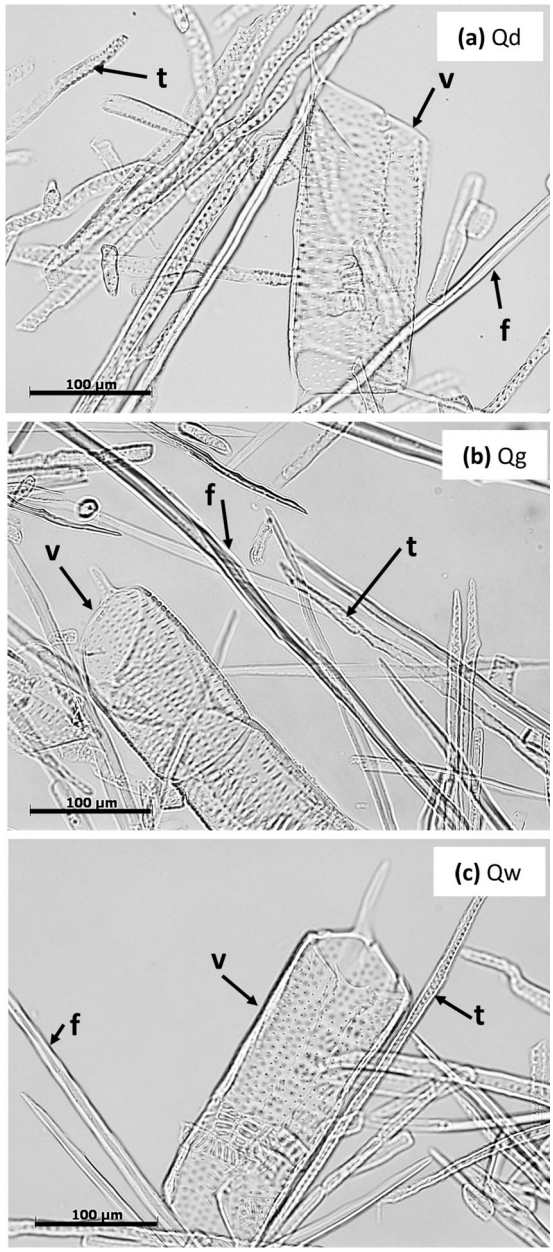

Figure 5. Representative micrographs of stem xylem macerations of three oak (*Quercus*) species, *Q. douglassii* (Qd), *Q. garryana* (Qg), and *Q. wislizeni* (Qw). Micrographs from all species are included in the Supplementary Material at 10.6084/m9.figshare.14380733. A scale bar is included in the lower-left corner of each panel. Within each panel, a representative vessel element (v), tracheid (t), and fiber (f) are identified.

vessels were of similar diameter to tracheids (Figure S5 in the Supplementary Material at 10.6084/m9.figshare.14380733), with overlap in the diameters of these conduit types.

The proportion of theoretical conductivity was calculated using the Hagen-Poiseuille relationship and measures of vessel and tracheid dimensions and abundance. These calculations indicated that tracheids account for an average of 10% of the theoretical conductivity in hydrated samples. This estimate varied by species due to differences in the structure and abundance of conduits as already described above. Among the species, the two diffuse-porous species, *Q. wislizeni* and *Q. chrysolepis*, were estimated to have the highest proportion of tracheid-based flow (15.5 ± 2.6 and 14.1 ± 3.2%), while the other species were lower (5.9 ± 1.0 for *Q. douglasii*, 6.6 ± 1.1 for *Q. garryana*, and 5.7 ± 1.3 % for *Q. kelloggii*).

Table 6.
Mean (± SE) conduit anatomical traits for five oak (*Quercus*) species in the Southern Sierra Nevada Mountains of California from sites at the high and low elevation distribution for each species.

Species	Dist.	*n*	Mean vessel lumen diameter (μm)	Dist.	Spp.	Max. vessel lumen diameter (μm)	Dist.	Spp.	Mean vessel length (cm)	Dist.	Spp.	Pit membrane area (μm²)	Dist.	Spp.	Tracheid diameter (μm)	Dist.	Spp.	Tracheid length (μm)	Dist.	Spp.
Q. chrysolepis	High	6	29.0 ± 1.1	n.s.	B	60.3 ± 1.6	n.s.	B	19.6 ± 1.7	n.s.	A	30.0 ± 1.5	n.s.	AB	13.0 ± 0.4	*	B	450.1 ± 15.2	*	AB
	Low	6	27.9 ± 1.3			66.2 ± 4.6			22.7 ± 1.1			28.8 ± 1.9			11.5 ± 0.3			417.2 ± 13.4		
Q. douglasii	High	6	32.0 ± 0.8	n.s.	A	82.0 ± 5.6	n.s.	A	13.7 ± 3.2	n.s.	B	31.3 ± 3.4	n.s.	A	13.5 ± 0.5	n.s.	A	412.8 ± 19.3	n.s.	B
	Low	6	32.2 ± 1.9			82.1 ± 4.9			10.1 ± 0.9			28.3 ± 1.0			14.4 ± 0.6			369.4 ± 23.7		
Q. garryana	High	6	32.7 ± 1.3	n.s.	A	85.8 ± 3.3	n.s.	A	12.8 ± 1.0	n.s.	B	26.6 ± 0.8	n.s.	AB	14.7 ± 0.4	n.s.	A	431.3 ± 13.6	n.s.	AB
	Low	6	29.5 ± 1.4			88.3 ± 5.0			12.1 ± 2.3			30.8 ± 2.0			14.6 ± 0.4			444.6 ± 15.5		
Q. kelloggii	High	6	34.1 ± 2.5	n.s.	A	97.7 ± 6.5	n.s.	A	9.4 ± 1.5	n.s.	B	25.5 ± 1.4	n.s.	B	14.1 ± 0.6	n.s.	A	389.5 ± 12.6	n.s.	B
	Low	6	34.0 ± 1.4			91.1 ± 6.9			13.1 ± 1.9			24.0 ± 1.0			13.2 ± 0.4			404.5 ± 14.1		
Q. wislizeni	High	6	27.8 ± 1.0	n.s.	B	65.6 ± 3.5	n.s.	B	11.1 ± 2.7	n.s.	B	27.0 ± 1.7	n.s.	AB	13.9 ± 0.4	n.s.	A	481.7 ± 15.7	n.s.	A
	Low	6	27.1 ± 2.2			65.3 ± 3.1			15.4 ± 1.5			27.3 ± 1.6			14.7 ± 0.6			438.6 ± 14.7		

To the right of each column comparisons between high and low sites for a species are presented (Dist.), with n.s. indicating no difference and an asterisk (*) indicating a difference ($P < 0.05$) between high and low sites. Results are also reported for a comparison of species values (Spp.) for each trait; different letters indicate significant differences among species.

Table 7.
Mean (± 1 SE) proportions of conduit (vessel elements and tracheids) and fiber cells from xylem tissue macerations for five oak (*Quercus*) species from sites at the high and low elevation distribution (Dist.) for each species.

Species	Dist.	*n*	Vessel elements (%)	Dist.	Spp.	Tracheids (%)	Dist.	Spp.	Fibers (%)	Dist.	Spp.
Q. chrysolepis	High	5	3.3 ± 0.4	n.s.	A	15.1 ± 2.4	n.s.	BC	81.6 ± 2.4	n.s.	AB
	Low	4	4.2 ± 0.9			16.0 ± 1.0			79.8 ± 0.5		
Q. douglasii	High	5	3.4 ± 0.7	n.s.	A	12.7 ± 2.2	n.s.	C	83.9 ± 2.8	n.s.	A
	Low	6	4.0 ± 0.6			12.6 ± 1.6			83.4 ± 2.0		
Q. garryana	High	6	4.6 ± 0.6	n.s.	A	18.9 ± 0.8	n.s.	ABC	76.5 ± 1.0	n.s.	ABC
	Low	6	4.3 ± 0.5			15.6 ± 1.8			80.1 ± 1.8		
Q. kelloggii	High	5	4.5 ± 0.4	n.s.	A	22.4 ± 2.6	n.s.	A	73.1 ± 2.5	n.s.	C
	Low	4	5.0 ± 0.4			21.6 ± 3.3			73.4 ± 3.4		
Q. wislizeni	High	6	3.9 ± 0.6	n.s.	A	17.4 ± 1.7	n.s.	AB	78.7 ± 1.8	n.s.	BC
	Low	4	3.0 ± 0.6			17.7 ± 2.9			79.3 ± 3.3		

To the right of each column comparisons between high and low sites for a species are presented (Dist.), with n.s. indicating no difference and an asterisk (*) indicating a difference ($P < 0.05$) between high and low sites. Results are also reported for a comparison of species values (Spp.) for each trait; different letters indicate significant differences among species.

Relationships between hydraulic structure and function

Hydraulic structural and functional traits were correlated with one another (Table S3 in the Supplementary Material at 10.6084/m9.figshare.14380733). Vulnerability to embolism (P_{50} and P_{90}) was correlated to K_s, with increased vulnerability in species with higher conductivity. Hydraulic traits, including P_{50}, P_{90}, and K_s, were correlated with vessel structure, including both mean and maximum vessel diameter. The proportion of fibers and tracheids within the xylem were inversely correlated to one another, but tracheid abundance was not correlated to vessel element abundance. Specific leaf area (SLA) was correlated to many xylem traits, including P_{50}, P_{90}, K_s, and vessel diameter.

DISCUSSION

Hydraulic function of tracheids in the xylem of vessel-bearing plants

Tracheids are likely important in maintaining hydraulic function during water stress, consistent with the hypothesized role of tracheids within the xylem of vessel-bearing angiosperm species in arid environments (Carlquist 1985; Carlquist & Hoekman 1985; Pratt *et al.* 2015). Tracheids appeared to be more resistant to water-stress induced embolism than vessels based on multiple lines of evidence, including (1) hydraulic conductivity was still measurable at pressures that were more negative than vessels could tolerate (described more below), and (2) micro-CT showed that tracheids were still water-filled and conductive when most vessels were already embolized. In hydrated stems, theoretical conductivity calculations suggest that tracheids account for an average of 10% of flow; however, the combination of vulnerable vessels with short functional lifespans and resistant tracheids with multiple years of function would result in tracheids becoming substantially more important in their hydraulic contribution than this calculation suggests. The hydraulic function of oaks, especially of older stems, can likely only be understood with increased knowledge of tracheid function.

It is often assumed that only the most current xylem growth rings are hydraulically conductive, particularly in deciduous species that drop their leaves, and for ring-porous species growing in cold environments where freeze-thaw stress would cause emboli to form within large diameter vessels (Jacobsen *et al.* 2018). However, for tracheids and latewood vessels, function may be maintained in older growth rings. This could particularly be the case in species with inter-conduit pit connections across growth rings (Kitin *et al.* 2009). In the present study, the iohexol sap flow tracer we used showed that tracheids were conductive in up to 7-year-old xylem in *Q. kelloggii*. Since the tracer was introduced to the base of a large branch and transpiration pulled the tracer through the xylem, tracer in these older tracheids suggests that older rings are functional in the plant and that they are part of a hydraulic pathway that connects older xylem to current-year leaves (Pratt *et al.* 2020a). This is an interesting result that suggests a novel role for tracheids as long-term functioning tracheary elements. This contrasts with vessels, which were not functional in any of the older growth rings and also often contained tyloses. These results are consistent with sap flow measures on an oak species that showed that large diameter vessels had a short functional lifespan and were only functional in the current year xylem, but low levels of flow occurred in several growth rings through smaller conduits (Granier *et al.* 1994).

Tracheids may be important in maintaining water transport following freeze-thaw conditions. Species differed in the proportion of tracheids and fibers in their xylem, but not in the proportion of vessel elements. Species that had higher tracheid abundance had reduced fiber abundance, indicating that there was a tradeoff in the presence of these two cell types. *Quercus douglasii* showed the lowest tracheid presence and occurred in the warmest and most water-limited sites along the transect for this study. The species with the highest tracheid abundance was *Q. kelloggii*, which occurred at the highest elevation site that regularly experiences winter freezing and receives abundant snowfall. High tracheid presence in this species may be advantageous because the narrow lumen diameters of tracheids makes them relatively resistant to freeze-thaw associated embolism formation (Davis *et al.* 1999; Pittermann & Sperry 2003, 2006).

Vessels were vulnerable to embolism

Data from multiple independent methods, including hydraulic vulnerability curves, micro-CT images, and SVAI, suggested that oak vessels were highly vulnerable to embolism. Nearly all vessels were embolized within micro-CT images of branches at native water potentials. Large numbers of embolized vessels within samples that were at water potentials between −2 and −4 MPa (the water potential range that we measured in plants during the dry season) suggests that very few vessels would remain functional within the xylem through the summer season.

Relatively vulnerable xylem has previously been found in several other studies on the same species using a variety of methods. *Quercus wislizeni* has been included in several studies that have shown rapid declines in conductivity with water stress, including studies using air injection (Matzner *et al.* 2001), both short and long stem segment lengths using the standard centrifuge technique (Jacobsen *et al.* 2007a; Tobin *et al.* 2013), and benchtop dehydration and acoustic emissions (Tobin *et al.* 2013). *Quercus douglasii* was recently examined using both micro-CT and benchtop dehydration (Pratt *et al.* 2020a) with samples showing high vulnerability to embolism, especially for older stems, although methods differed from one another in their specific estimates. *Quercus garryana* seedlings have been shown to have relatively large losses in conductivity with moderate water stress, although this study was not on the same subspecies that we examined (Merz *et al.* 2017).

Large seasonal losses in conductivity may be part of a hydraulic strategy in highly seasonal environments, with selection that maximizes conductivity during a short period of a high productivity followed by limited water use and traits that permit tolerance of low conductivity. High seasonal embolism has been described previously for some species and organs, particularly in arid and semi-arid environments (Sperry & Hacke 2002; Domec *et al.* 2006; Jacobsen *et al.* 2007b; de Dios Miranda *et al.* 2010). Additionally, high seasonal levels of embolism have been described previously for some oak species (Sperry *et al.* 1994; Tognetti *et al.* 1999; Nardini & Pitt 1999; Nardini *et al.* 2013). There is also good evidence that oaks can refill xylem and we do not rule this out (Taneda & Sperry 2008); however, such refilling would be futile during the dry season and likely impossible due to sustained negative hydrostatic xylem pressure in the mediterranean-type environment in which we sampled. Vessels could also serve as a water storage reservoir, with water released as vessels embolize (Yazaki *et al.* 2020).

Fatigue does not explain the vulnerability of current-year xylem

For some species, older vessels may become more vulnerable to embolism through a process termed 'fatigue' (Hacke *et al.* 2001). This may be relevant for the present study because we examined stem samples that were around 6 years in age and would have included older xylem. We examined the potential influence of fatigue on our curves by measuring stems in which the older rings had been sealed and only the current year's growth was included in hydraulic measures (Rodríguez-Zaccaro *et al.* 2019). Vessels grown within the current year would not have experienced either the water stress of the dry season or freeze-thaw stress of winter. The vulnerability curves produced by these stems were similar to curves measured on samples that included all their growth rings.

Examination of the current year growth of several-year-old branches, such as within the present study, is not comparable to measures of younger stems that only contain a single year of growth. Young stems display diffuse-porous xylem in oaks. In ring-porous species, the current-year xylem produced in older stems differs and may contain much larger vessels as the vascular cambium transitions to forming ring-porous mature xylem (Pratt *et al.* 2020a). This may be one reason why our resistance to embolism estimates differed from a recent study that examined only young narrow stems (Skelton *et al.* 2018). Some studies have found that 1-year old stems are more resistant (Nolf *et al.* 2017). Probably more important, it has been established that different methods can yield different vulnerability estimates, and comparing across studies using different methods is not straightforward (Venturas *et al.* 2019; Pratt *et al.* 2020a, b).

SVAI confirmed that current-year vessels were quite vulnerable to air-seeding. The SVAI curve, which only measures air-seeding of vessels and not tracheids, was more vulnerable than the hydraulic curve measured on paired samples. The hydraulic vulnerability curve, which was still quite vulnerable but showed a low level of conductivity at more negative water

potentials, included conductivity through both tracheids and vessels. Thus, the difference between these curves of current-year xylem was likely due to the hydraulic contribution of more resistant tracheids that were included in hydraulic measures but not in SVAI measures.

There has been debate about methods to measure plant hydraulic function and one important factor has been whether emboli are removed prior to beginning curves, with some labs flushing out emboli while others do not flush (discussed in Hacke *et al.* 2015). We flushed to remove emboli prior to initiating hydraulic measures, which has the benefit of standardizing our methods with prior studies on some of the same species that have used native measures and benchtop dehydration techniques, which compare native to flushed conductivity values (Jacobsen *et al.* 2007a; Tobin *et al.* 2013; Pratt *et al.* 2020a). Flushing out emboli will refill some vessels that were not functional in intact plants and some that may be damaged or fatigued. To correct for this, we set the maximum conductivity used to evaluate vulnerability curves as the conductivity following a −0.5 MPa treatment, which is the approximate water potential of hydrated tissues during the winter/spring wet season. This type of correction has been used previously to compensate for fatigue (Hacke *et al.* 2000; Tobin *et al.* 2013). The rationale for this is that any vessels and tracheids that were damaged would easily air-seed and would therefore embolize following this relatively minor pressure treatment. It is possible that some vessels that are refilled by flushing will be damaged, but not so severely that they embolize at −0.5 MPa, but this has never been tested. In the present study, vulnerability curve shapes were similar in multi-year and current-year only measures, suggesting neither flushing nor fatigue were likely causing large effects and would not generally change the interpretation of our results.

Methods comparisons in a tracheid-vessel network

A recent model of xylem hydraulic function predicted that species with highly connected conduit networks, such as those found in vessel-bearing xylem that also contains tracheids, would exhibit greater agreement between micro-CT and hydraulic methods (Jacobsen & Pratt 2018b based on the model presented by Mrad *et al.* 2018). Our results support this prediction and micro-CT and hydraulic PLC estimates agreed in our samples. Tracheids increase the number and pathways of connections between conduits and may reduce the likelihood of pit limitation or isolated xylem sectors that may lead to discrepancies in other species. This result contrasts with recent studies on other species that have found that micro-CT analyses often diverge from hydraulic measures, particularly at the dry end of the curve when conductivity goes to zero, but some vessels still contain fluid (Nolf *et al.* 2017; Jacobsen *et al.* 2019; Venturas *et al.* 2019; Pratt *et al.* 2020a, b). It may be that the agreement that we found was due to our samples containing high levels of embolism and micro-CT and hydraulic estimates at intermediate embolism levels may still diverge as recently found for *Quercus douglasii* (Pratt *et al.* 2020a).

Hydraulic function and structure

Across oak species, there were many differences in xylem function and structural traits, illustrating the variety of traits found within this diverse genus (Cavender-Bares 2019). *Quercus wislizeni*, an evergreen shrub whose distribution was limited to lower elevations, was the most resistant to embolism. The most vulnerable species with the highest K_s were *Q. garryana* and *Q. kelloggii*, both deciduous trees with middle and upper elevation distributions in this study. These differences were part of a general trend of differences between evergreen-diffuse porous and deciduous-ring porous species in both their hydraulic function and xylem structure (Cavender-Bares & Holbrook 2001).

Hydraulic function, including P_{50} and K_s, was correlated with xylem structure. Vessel diameter was strongly correlated with both P_{50} and K_s, with larger vessels correlated with increased vulnerability to embolism and higher hydraulic transport efficiency, as has often been reported (Martínez-Vilalta *et al.* 2002; Wheeler *et al.* 2005; Hacke *et al.* 2006; Jacobsen *et al.* 2007a). P_{50} and K_s were correlated, with the most resistant species also having the lowest conductivity, and consistent with hypothesized trade-offs between hydraulic safety and efficiency (reviewed in Venturas *et al.* 2017).

The oak species included in the present study did not generally differ in xylem structure and function between their upper and lower elevation distribution limits along our experimental transect. Species may have limited variability in the traits that we examined, which may reduce their ability to respond to changing climates, although the same may not be the case for other oak species (Jacobsen *et al.* 2014; Ramírez-Valiente & Cavender-Bares 2017). In the southern Sierra Nevada, individuals occurring at the dry ends of distributions (i.e., low elevation) may be particularly threatened and some mortality has already been observed in our studied species, especially *Q. douglasii* (Brown *et al.* 2018; Batllori *et al.* 2020). In addition, we observed extensive dieback and some mortality at our lowest elevation site for both *Q. douglasii* and *Q. wislizeni* (Fig. S6 in the Supplementary Material at 10.6084/m9.figshare.14380733).

Limited within-species variability may partially explain the high species diversity along our experimental transect over a relatively short distance (ca. 10 km). If species are not able to plastically adjust to different conditions, they may be more limited in their potential habitats leading to narrow distributions and higher turnover among oak species. Previous studies

have found variable evidence for intra-specific variation in hydraulic function. Several studies have found that species may vary greatly in their conductivity and embolism resistance among populations and seasonally (Mencuccini & Comstock 1997; Kavanagh *et al.* 1999; Kolb & Sperry 1999; Sparks & Black 1999; Jacobsen *et al.* 2007b; Herbette *et al.* 2010; Jacobsen *et al.* 2014; Kilgore *et al.* 2020). Other studies have found that embolism resistance changes with growing conditions (Awad *et al.* 2010; Hacke *et al.* 2010; Wortemann *et al.* 2011). In contrast, other studies have found limited intra-specific variability in these traits (Jacobsen & Pratt 2013; Lamy *et al.* 2011; González-Muñoz *et al.* 2018; Jinagool *et al.* 2018; Ramirez *et al.* 2020), such as was found in the present study.

CONCLUSIONS

Many angiosperm taxa contain both vessels and tracheids. We used *Quercus* to examine the effects that the environment may have on how plants transport water through both vasicentric tracheids and vessels. *Quercus* species in California occupy a wide range of habitats and elevations and exist in diverse forms, varying phenology, leaf habit (evergreen, drought deciduous, winter deciduous), plant habit (tree, shrub), and growth ring porosity (ring, diffuse). Oak species are culturally and economically important and dominate many northern hemisphere plant communities. One question that has long been of interest is the evolution of vessels from tracheid-bearing ancestors, an additional question is why some species re-evolved tracheids (Wheeler & Bass 2018). Studies of the functional roles of these conduits types when they co-occur may be important in understanding the evolution of cellular division of labor within the xylem.

ACKNOWLEDGEMENTS

L. Maynard Moe is thanked for comments on an early manuscript draft and for serving on the M.S. Biology Thesis Committee of M.I.P. Two anonymous reviewers are thanked for their constructive and thorough comments, which greatly improved this manuscript. Aaron Baumgardner, Mitchell Coleman, Jessica Valdovinos, and Viridiana Castro are thanked for their assistance with field and with anatomical measures. NSF CREST HRD-1547784 and NSF CAREER IOS-1252232 are acknowledged for support.

REFERENCES

Alder NN, Pockman WT, Sperry JS, Nuismer S. 1997. Use of centrifugal force in the study of xylem cavitation. J. Exp. Bot. 48: 665–674. DOI: 10.1093/jxb/48.3.665.

Allen CD, Macalady AK, Chenchouni H, Bachelet D, Mcdowell N, Vennetier M, Kitzberger T, Rigling A, Breshears DD, Hogg EH, Gonzalez P, Fensham R, Zhang Z, Castro J, Demidova N, Lim J-H, Allard G, Running SW, Semerci A, Cobb N. 2010. A global overview of drought and heat-induced tree mortality reveals emerging climate change risks for forests. Forest Ecol. Manage. 259: 660–684. DOI: 10.1016/j.foreco.2009.09.001.

Anderegg WRL, Klein T, Bartlett M, Sack L, Pellegrin AFA, Choat B, Jansen S. 2016. Meta-analysis reveals that hydraulic traits explain cross-species patterns of drought-induced tree mortality across the globe. Proc. Natl. Acad. Sci. USA 113: 5024–5029. DOI: 10.1073/pnas.1525678113.

Awad H, Barigah T, Badel E, Cochard H, Herbette S. 2010. Poplar vulnerability to xylem cavitation acclimates to drier soil conditions. Physiol. Plant. 139: 280–288. DOI: 10.1111/j.1399-3054.2010.01367.x.

Baas P. 1986. Terminology of imperforate tracheary elements — in defence of libriform fibres with minutely bordered pits. IAWA J. 7: 82–86. DOI: 10.1163/22941932-90000446.

Baldwin BG, Goldman DH, Keil DJ, Patterson R, Rosatti TJ, Wilken DH (eds). 2012. The jepson manual: vascular plants of California. University of California Press, Berkeley, CA.

Barotto AJ, Fernandez ME, Gyenge J, Meyra A, Martinez-Meier A, Monteoliva S. 2016. Tree Phys. 36: 1485–1497. DOI: 10.1093/treephys/tpw072.

Batllori E, Lloret F, Aakala T, Anderegg WRL, Aynekulu E, et al. 2020. Forest and woodland replacement patterns following drought-induced mortality. Proc. Natl. Acad. Sci. USA 117: 29720–29729. DOI: 10.1073/pnas.2002314117.

Brown BJ, McLaughlin BC, Blakey RV, Morueta-Holme N. 2018. Future vulnerability mapping based on response to extreme climate events: dieback thresholds in an endemic California oak. Diversity and Distributions 24: 1186–1198. DOI: 10.1111/ddi.12770.

Cai J, Tyree MT. 2010. The impact of vessel size on vulnerability curves: data and models for within-species variability in saplings of aspen, *Populus tremuloides* Michx. Plant Cell Environ. 33: 1059–1069. DOI: 10.1111/j.1365-3040.2010.02127.x.

Carlquist S. 1985. Vasicentric tracheids as a drought survival mechanism in the woody flora of southern California and similar regions; review of vasicentric tracheids. Aliso 11: 37–68. DOI: 10.5642/aliso.19851101.05.

Carlquist S. 1986. Terminology of imperforate tracheary elements. IAWA J. 7: 75–81. DOI: 10.1163/22941932-90000445.

Carlquist S, Hoekman DA. 1985. Ecological wood anatomy of the woody southern California flora. IAWA J. 6: 319–347. DOI: 10.1163/22941932-90000960.

Cavender-Bares J. 2019. Diversification, adaptation, and community assembly of the American oaks (*Quercus*), a model clade for integrating ecology and evolution. New Phytol. 221: 669–692. DOI: 10.1111/nph.15450.

Cavender-Bares J, Holbrook NM. 2001. Hydraulic properties and freezing-induced cavitation in sympatric evergreen and deciduous oaks with contrasting habitats. Plant Cell Environ. 24: 1243–1256. DOI: 10.1046/j.1365-3040.2001.00797.x.

Davis SD, Sperry JS, Hacke UG. 1999. The relationship between xylem conduit diameter and cavitation caused by freezing. Am. J. Bot. 86: 1367–1372. DOI: 10.2307/2656919.

de Dios Miranda J, Padilla FM, Martínez-Vilalta J, Pugnaire FI. 2010. Woody species of a semi-arid community are only moderately resistant to cavitation. Funct. Plant Biol. 37: 828–839. DOI: 10.1071/FP09296.

Domec JC, Scholz FG, Bucci SJ, Meinzer FC, Goldstein G, Villalobos-Vega R. 2006. Diurnal and seasonal variation in root xylem embolism in Neotropical savanna woody species: impact on stomatal control of plant water status. Plant Cell Environ. 29: 26–35. DOI: 10.1111/j.1365-3040.2005.01397.x.

Franklin GL. 1945. Preparation of thin sections of synthetic resins and wood-resin composites, and a new macerating method for wood. Nature 155: 51–59. DOI: 10.1038/155051a0.

González-Muñoz N, Sterck F, Torres-Ruiz JM, Petit G, Cochard H, von Arx G, Lintunen A, Caldeira MC, Capdeville G, Copini P, Gebauer R. 2018. Quantifying *in situ* phenotypic variability in the hydraulic properties of four tree species across their distribution range in Europe. PLoS ONE 13: 1–17. DOI: 10.1371/journal.pone.0196075.

Granier A, Anfodillo T, Sabatti M, Cochard H, Dreyer E, Tomasi M, Valentini R, Breda N. 1994. Axial and radial water flow in the trunks of oak trees: a quantitative and qualitative analysis. Tree Physiol. 14: 1383–1396. DOI: 10.1093/treephys/14.12.1383.

Hacke UG, Plavcová L, Almeida-Rodriguez A, King-Jones S, Zhou W, Cooke JE. 2010. Influence of nitrogen fertilization on xylem traits and aquaporin expression in stems of hybrid poplar. Tree Physiol. 30: 1016–1025. DOI: 10.1093/treephys/tpq058.

Hacke UG, Sperry JS, Pittermann J. 2000. Drought experience and cavitation resistance in six shrubs from the Great Basin, Utah. Basic Appl. Ecol. 1: 31–41. DOI: 10.1078/1439-1791-00006.

Hacke UG, Sperry JS, Wheeler JK, Castro L. 2006. Scaling of angiosperm xylem structure with safety and efficiency. Tree Physiol. 26: 689–701. DOI: 10.1093/treephys/26.6.689.

Hacke UG, Stiller V, Sperry JS, Pittermann J, McCulloh KA. 2001. Cavitation fatigue. Embolism and refilling cycles can weaken the cavitation resistance of xylem. Plant Physiol. 125: 779–786. DOI: 10.1104/pp.125.2.779.

Hacke UG, Venturas MD, MacKinnon ED, Jacobsen AL, Sperry JS, Pratt RB. 2015. The standard centrifuge method accurately measures vulnerability curves of long-vesselled olive stems. New Phytol. 205: 116–127. DOI: 10.1111/nph.13017.

Hargrave KR, Kolb KJ, Ewers FW, Davis SD. 1994. Conduit diameter and drought-induced embolism in *Salvia mellifera* Greene (Labiatae). New Phytol. 126: 695–705. DOI: 10.1111/j.1469-8137.1994.tb02964.x.

Herbette S, Wortemann R, Awad H, Huc R, Cochard H, Barigah TS. 2010. Insights into xylem vulnerability to cavitation in *Fagus sylvatica* L.: phenotypic and environmental sources of variability. Tree Physiol. 30: 1448–1455. DOI: 10.1093/treephys/tpq079.

Jacobsen AL, Pratt RB. 2013. Vulnerability to cavitation of central California *Arctostaphylos* (Ericaceae): a new analysis. Oecologia 171: 329–334. DOI: 10.1007/s00442-012-2414-9.

Jacobsen AL, Pratt RB. 2018a. Extensive drought-associated plant mortality as an agent of type-conversion in chaparral shrublands. New Phytol. 219: 498–504. DOI: 10.1111/nph.15186.

Jacobsen AL, Pratt RB. 2018b. Going with the flow: structural determinants of vascular tissue transport efficiency and safety. Plant Cell Environ. 41: 2715–2717. DOI: 10.1111/pce.13446.

Jacobsen AL, Pratt RB, Davis SD, Ewers FW. 2007b. Cavitation resistance and seasonal hydraulics differ among three arid Californian plant communities. Plant Cell Environ. 30: 1599–1609. DOI: 10.1111/j.1365-3040.2007.01729.x.

Jacobsen AL, Pratt RB, Davis SD, Tobin MF. 2014. Geographic and seasonal variation in chaparral vulnerability to cavitation. Madroño 61: 317–328. DOI: 10.3120/0024-9637-61.4.317.

Jacobsen AL, Pratt RB, Ewers FW, Davis SD. 2007a. Cavitation resistance among twenty-six chaparral species of southern California. Ecol. Monogr. 77: 99–115. DOI: 10.1890/05-1879.

Jacobsen AL, Pratt RB, Venturas MD, Hacke UG. 2019. Large volume vessels are vulnerable to water-stress-induced embolism in stems of poplar. IAWA J. 40: 4–22. DOI: 10.1163/22941932-40190233.

Jacobsen AL, Tobin MF, Toschi HS, Percolla MI, Pratt RB. 2016. Structural determinants of increased susceptibility to dehydration-induced cavitation in post-fire resprouting chaparral shrubs. Plant Cell Environ. 39: 2473–2485. DOI: 10.1111/pce.12802.

Jacobsen AL, Valdovinos-Ayala J, Pratt RB. 2018. Functional lifespans of xylem vessels: development, hydraulic function, and post-function of vessels in several species of woody plants. Am. J. Bot. 105: 142–150. DOI: 10.1002/ajb2.1029.

Jinagool W, Lamacque L, Delmas M, Delzon S, Cochard H, Herbette S. 2018. Is there variability for xylem vulnerability to cavitation in walnut tree cultivars and species (*Juglans* spp.)? HortScience 53: 132–137. DOI: 10.21273/HORTSCI12350-17.

Kavanagh KL, Bond BJ, Aitken SN, Gartner BL, Knowe S. 1999. Shoot and root vulnerability to xylem cavitation in four populations of Douglas-fir seedlings. Tree Physiol. 19: 31–37. DOI: 10.1093/treephys/19.1.31.

Kilgore JS, Jacobsen AL, Telewski FW. 2020. Hydraulics of *Pinus* (subsection Ponderosae) populations across an elevation gradient in the Santa Catalina Mountains of southern Arizona. Madroño 67: 218–226.

Kitin P, Fujii T, Abe H, Takata K. 2009. Anatomical features that facilitate radial flow across growth rings and from xylem to cambium in *Cryptomeria japonica*. Ann. Bot. 103: 1145–1157. DOI: 10.1093/aob/mcp050.

Kolb KJ, Sperry JS. 1999. Transport constraints on water use by the Great Basin shrub, *Artemisia tridentata*. Plant Cell Environ. 22: 925–936. DOI: 10.1046/j.1365-3040.1999.00458.x.

Lamy JB, Bouffier L, Burlett R, Plomion C, Cochard H, Delzon S. 2011. Uniform selection as a primary force reducing population genetic differentiation of cavitation resistance across a species range. PloS One 6: 1–12. DOI: 10.1371/journal.pone.0023476.

Martínez-Vilalta J, Prat E, Oliveras I, Piñol J. 2002. Xylem hydraulic properties of roots and stems of nine Mediterranean woody species. Oecologia 133: 19–29. DOI: 10.1007/s00442-002-1009-2.

Matzner SL, Rice KJ, Richards JH. 2001. Intra-specific variation in xylem cavitation in interior live oak (*Quercus wislizenii* A. DC.). J. Exp. Bot. 52: 783–789. DOI: 10.1093/jexbot/52.357.783.

Mencuccini M, Comstock J. 1997. Vulnerability to cavitation in populations of two desert species, *Hymenoclea salsola* and *Ambrosia dumosa*, from different climatic regions. J. Exp. Bot. 48: 1323–1334. DOI: 10.1093/jxb/48.6.1323.

Merz MA, Donahue RA, Poulson ME. 2017. Physiological response of Garry oak (*Quercus garryana*) seedlings to drought. Northwest Sci. 91: 140–159. DOI: 10.3955/046.091.0206.

Mrad A, Domec JC, Huang C-W, Frederic L, Katul G. 2018. A network model links wood anatomy to xylem tissue hydraulic behavior and vulnerability to cavitation. Plant Cell Environ. DOI: 10.1111/pce.13415.

Nardini A, Battistuzzo M, Savi T. 2013. Shoot desiccation and hydraulic failure in temperate woody angiosperms during an extreme summer drought. New Phytol. 200: 322–329. DOI: 10.1111/nph.12288.

Nardini A, Pitt F. 1999. Drought resistance of *Quercus pubescens* as a function of root hydraulic conductance, xylem embolism and hydraulic architecture. New Phytol. 143: 485–493. DOI: 10.1046/j.1469-8137.1999.00476.x.

Nolf M, Lopez R, Peters JM, Flavel RJ, Koloadin LS, Young IM, Choat B. 2017. Visualization of xylem embolism by X-ray microtomography: a direct test against hydraulic measurements. New Phytol. 214: 890–898. DOI: 10.1111/nph.14462.

Olson M, Rosell JA, Martínez-Pérez C, León-Gómez C, Fajardo A, Isnard S, Cervantes-Alcayde MA, Echeverría A, Figueroa-Abundiz VA, Segovia-Rivas A, Trueba S. 2020. Xylem vessel-diameter–shoot-length scaling: ecological significance of porosity types and other traits. Ecol. Monogr. 90: e01410. DOI: 10.1002/ecm.1410.

Olson ME, Rosell JA. 2013. Vessel diameter–stem diameter scaling across woody angiosperms and the ecological causes of xylem vessel diameter variation. New Phytol. 197: 1204–1213. DOI: 10.1111/nph.12097.

Paddock III WAS, Davis SD, Pratt RB, Jacobsen AL, Tobin MF, Lopez-Portillo J, Ewers FW. 2013. Factors determining mortality of adult chaparral shrubs in an extreme drought year in California. Aliso 31: 49–57. DOI: 10.5642/aliso.20133101.08.

Pittermann J, Sperry JS. 2003. Tracheid diameter is the key trait determining the extent of freezing-induced embolism in conifers. Tree Physiol. 23: 907–914. DOI: 10.1093/treephys/23.13.907.

Pittermann J, Sperry JS. 2006. Analysis of freeze-thaw embolism in conifers. The interaction between cavitation pressure and tracheid size. Plant Physiol. 140: 374–382. DOI: 10.1104/pp.105.067900.

Pratt RB, Castro V, Fickle JC, Jacobsen AL. 2020a. Embolism resistance of different aged stems of a California oak species (*Quercus douglasii*): optical and micro-CT methods differ from the benchtop-dehydration standard. Tree Physiol. 40: 5–18. DOI: 10.1093/treephys/tpz092.

Pratt RB, Castro V, Fickle JC, Madsen A, Jacobsen AL. 2020b. Factors controlling drought resistance in grapevine (*Vitis vinifera*, chardonnay): application of a new micro CT method to assess functional embolism resistance. Am. J. Bot. 107: 618–627. DOI: 10.1002/ajb2.1450.

Pratt RB, Jacobsen AL. 2018. Identifying which conduits are moving water in woody plants: a new HRCT-based method. Tree Physiol. 38: 1200–1212. DOI: 10.1093/treephys/tpy034.

Pratt RB, Percolla MI, Jacobsen AL. 2015. Integrative xylem analysis of chaparral shrubs. In: Hacke UG (ed.), Functional and ecological xylem anatomy: 189–207. Springer, Berlin. DOI: 10.1007/978-3-319-15783-2_7.

Ramirez AR, De Guzman ME, Dawson TE, Ackerly DD. 2020. Plant hydraulic traits reveal islands as refugia from worsening drought. Conserv. Physiol. 8: coz115. DOI: 10.1093/conphys/coz115.

Ramírez-Valiente JA, Cavender-Bares J. 2019. Evolutionary trade-offs between drought resistance mechanisms across a precipitation gradient in a seasonally dry tropical oak (*Quercus oleoides*). Tree Physiol. 37: 889–901. DOI: 10.1093/treephys/tpx040.

Rodríguez-Zaccaro FD, Valdovinos-Ayala J, Percolla MI, Venturas MD, Pratt RB, Jacobsen AL. 2019. Wood structure and function change with maturity: age of the vascular cambium is associated with xylem changes in current-year growth. Plant Cell Environ. 42: 1816–1831. DOI: 10.1111/pce.13528.

Rosell JA, Olson ME, Aguirre-Hernandez R, Carlquist S. 2007. Logistic regression in comparative wood anatomy: tracheid types, wood anatomical terminology, and new inferences from the Carlquist and Hoekman southern Californian data set. Bot. J. Linn. Soc. 154: 331–351. DOI: 10.1111/j.1095-8339.2007.00667.x.

Skelton RP, Dawson TE, Thompson SE, Shen Y, Weitz AP, Ackerly D. 2018. Low vulnerability to xylem embolism in leaves and stems of North American oaks. Plant Physiol. 177: 1066–1077. DOI: 10.1104/pp.18.00103.

Sparks JP, Black RA. 1999. Regulation of water loss in populations of *Populus trichocarpa*: the role of stomatal control in preventing xylem cavitation. Tree Physiol. 19: 453–459. DOI: 10.1093/treephys/19.7.453.

Sperry JS, Donnelly JR, Tyree MT. 1988. A method for measuring hydraulic conductivity and embolism in xylem. Plant Cell Environ. 11: 35–40. DOI: 10.1111/j.1365-3040.1988.tb01774.x.

Sperry JS, Hacke UG. 2002. Desert shrub water relations with respect to soil characteristics and plant functional type. Funct. Ecol. 16: 367–378. DOI: 10.1046/j.1365-2435.2002.00628.x.

Sperry JS, Hacke UG, Wheeler JK. 2005. Comparative analysis of end wall resistivity in xylem conduits. Plant Cell Environ. 28: 456–465. DOI: 10.1111/j.1365-3040.2005.01287.x.

Sperry JS, Nichols KL, Sullivan JE, Eastlack SE. 1994. Xylem embolism in ring-porous, diffuse-porous, and coniferous trees of northern Utah and interior Alaska. Ecology 75: 1736–1752. DOI: 10.2307/1939633.

Taneda H, Sperry JS. 2008. A case-study of water transport in co-occurring ring-versus diffuse-porous trees: contrasts in water-status, conducting capacity, cavitation and vessel refilling. Tree Physiol. 28: 1641–1651. DOI: 10.1093/treephys/28.11.1641.

Tobin MF, Pratt RB, Jacobsen AL, De Guzman ME. 2013. Xylem vulnerability to cavitation can be accurately characterized in species with long vessels using a centrifuge method. Plant Biol. 15: 496–504. DOI: 10.1111/j.1438-8677.2012.00678.x.

Tognetti R, Longobucco A, Raschi A. 1999. Seasonal embolism and xylem vulnerability in deciduous and evergreen Mediterranean trees influenced by proximity to a carbon dioxide spring. Tree Physiol. 19: 271–277. DOI: 10.1093/treephys/19.4-5.271.

Tyree MT, Zimmermann MH. 2002. Xylem structure and the ascent of sap. Springer, Berlin.
Venturas MD, MacKinnon ED, Dario HL, Jacobsen AL, Pratt RB, Davis SD. 2016. Chaparral shrub hydraulic traits, size and life history types relate to species mortality during California's historic drought of 2014. PLoS ONE 11: 1–22. DOI: 10.1371/journal.pone.0159145.
Venturas MD, Pratt RB, Jacobsen AL, Castro V, Fickle JC, Hacke UG. 2019. Direct comparison of four methods to construct xylem vulnerability curves: differences among techniques are linked to vessel network characteristics. Plant Cell Environ. 42: 2422–2436. DOI: 10.1111/pce.13565.
Venturas MD, Sperry JS, Hacke UG. 2017. Plant xylem hydraulics: what we understand, current research, and future challenges. J. Integr. Plant Biol. 59: 356–389. DOI: 10.1111/jipb.12534.
Wheeler EA, Baas P. 2018. Wood evolution: Baileyan trends and functional traits in the fossil record. IAWA J. 40: 488–529. DOI: 10.1163/22941932-40190230.
Wheeler JK, Sperry JS, Hacke UG, Hoang N. 2005. Inter-vessel pitting and cavitation in woody Rosaceae and other vesselled plants: a basis for a safety versus efficiency trade-off in xylem transport. Plant Cell Environ. 28: 800–812. DOI: 10.1111/j.1365-3040.2005.01330.x.
Wortemann R, Herbette S, Barigah TS, Fumanal B, Alia R, Ducousso A, Gomory D, Roeckel-Drevet P, Cochard H. 2011. Genotypic variability and phenotypic plasticity of cavitation resistance in *Fagus sylvatica* L. across Europe. Tree Physiol. 31: 1175–1182. DOI: 10.1093/treephys/tpr101.
Yazaki K, Levia DF, Takenouchi A, Watanabe M, Kabeya D, Miki NH, Taneda H, Ogasa MY, Oguro M, Saiki ST, Tobita H. 2020. Imperforate tracheary elements and vessels alleviate xylem tension under severe dehydration: insights from water release curves for excised twigs of three tree species. Am. J. Bot. 107: 1–14. DOI: 10.1002/ajb2.1518.

Edited by Veronica de Micco